JOINT INSTITUTE FOR NUCLEAR RESEARCH
Veksler and Baldin Laboratory of High Energy Physics

FINAL REPORT ON THE START PROGRAMME

Analysis of relativistic muon interactions with light nuclei using nuclear track emulsion method.

Supervisor:
Dr. Pavel Igorevich Zarubin

Student:
Ekaterina Khabarova, Russia
Peter the Great St.Petersburg Polytechnic University

Participation period:
June 30 – August 10,
Summer Session 2024

Dubna, 2024

Abstract

Fragmentation of nuclei induced by the of relativistic muons, the nuclear track emulsions method, in comparison with electron experiments, represents unique experimental material and provides complete observations in 4π-geometry, with complete identification of all charged fragments in each interaction event and precision measurements ranges (~0.5μ) and emitted angles (~10^{-3} rad) of secondary particles. The complete observation of particle tracks (starting from MIPs up to heavy low energy ions) is ensured by a low detection threshold of ~1 keV.

In the work carried out, events with the formation of 3 alpha particles as a consequence of electromagnetic dissociation of the excited target ^{12}C nucleus while the interaction with the relativistic muons. The real range of alpha particles were measured and their kinetic energies were reconstructed using simulation in the SRIM program.

1. Introduction

The first observations of fragmentation of atomic nuclei were observed in layers of nuclear photographic emulsion exposed by cosmic rays [1]. The study of fragmentation processes of target nuclei in nucleon-nucleus and nucleus-nucleus collisions at high energies attracts great interest at the present time [2-7]. An important role here is played by experiments to study nuclear fragmentation processes, which make it possible to extract significant information about the fragmentation mechanism and the cluster structure of fragmenting nuclei, which affects the cross section for the formation of fragments. Of particular interest in this regard are experimental studies of the fragmentation of nα nuclei, such as ^{12}C, ^{16}O etc., where the role of the alpha cluster structure dominates. The study of ensembles of several α-particles makes it possible to identify the role of unstable nuclei ^{8}Be and ^{9}B and search for their analogues, starting with the 3α-Hoyle state (HS) [8,9].

The figure 1 shows a diagram of the decay of a ^{12}C nucleus while interacting with a muon. This reaction occurs due to the exchange of a muon and a target nucleus with a virtual photon, followed by a transition to a vector meson or a pair of pseudoscalar mesons. The most probable branch of the ^{12}C(m,m')3α reaction goes through levels from 7.65 to 16 MeV below the threshold for the separation of single nucleons.

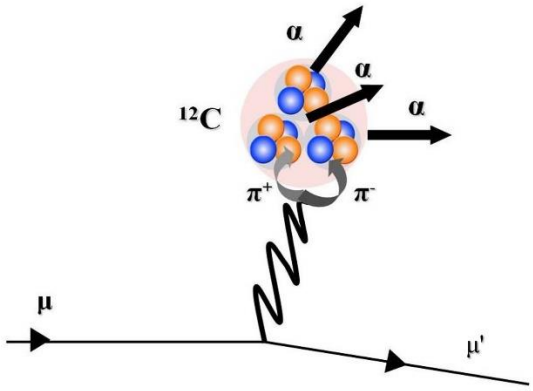

Figure 1. Diagram of the decay of a ^{12}C nucleus while interacting with a muon.

The cross section of discussed reaction is fundamentally important for geological assessments. Traditionally, the radioactive decay of uranium, thorium and their daughter radionuclides is indicated as a source of helium, and analysis for the presence of helium serves to search for their deposits. At the same time, the reaction $\mu + {}^{12}C \rightarrow \mu' + 3\alpha$ can serve as a mechanism for generating helium in natural gas deposits at kilometer depths, where cosmic muons with energies of hundreds of GeV can penetrate. In this case, there should be a direct relationship between the age of the deposit and the concentration of helium in it.

1. 1. Nuclear track emulsion method

1.1.1. Fundamentals of the process of latent image formation and manifestation.

Photoemulsion consists of individual crystals or grains of silver bromide (AgBr), on average evenly distributed in gelatin. The size and shape of the individual grains and their number per unit volume depend on the emulsion preparation technology. For example, increasing the crystallization time of AgBr leads to an increase in the average grain size and an increase in the photosensitivity of the layer. The grain size is of the order of 0.1-1 μm.

Normal light exposure or irradiation with ionizing radiation does not directly produce a visible effect on the silver halide grains, but it does make some grains capable of developing. These grains contain the latent image. The carrier of the latent image in each grain is a microscopic particle of metallic silver formed during exposure and located on or near the surface of the grain where it is accessible to the chemical developer. The probability of formation of a latent image by an ionizing particle passing through the grain is less than unity, especially if this particle is characterized by small ionization losses.

The exact nature of the formation of latent image centers is not clear. It is assumed that the primary electrons that originated along the track of the ionizing particle and passed through the silver bromide crystal, spend part of their energy to transfer electrons from the valence zone to the conduction zone. Once in the conduction zone and being able to move under the action of the electric field, these electrons are collected in the so-called sensitivity centers, which owe their origin to defects in the crystal lattice or impurity atoms. In the sensing center, electrons are trapped at levels located in the forbidden zone. An electron at such a level creates a local perturbation of the electric field, which attracts silver ions, which are not fixed in the silver bromide crystal lattice and are always present in some quantity in the AgBr crystal. At the center of sensitivity, the silver ions, attaching electrons to themselves, turn into atoms. If the number of silver atoms accumulated as a result of this process in the sensing center reaches several tens or hundreds, and the sensing center itself is located not too far from the crystal surface, a latent image is formed.

The manifestation of the latent image consists in the reduction of halide silver to metallic silver. In this case, the irradiated grains containing the latent image centers are reduced to atomic silver much faster than the unirradiated grains, because the latent image center (metallic silver) acts as an accumulation center for the silver released in the process of development. With prolonged development, the unirradiated grains also begin to recover, forming a veil. The veil is caused by the fact that the unirradiated grain may contain small groups of metallic silver atoms, which cause the reduction of all silver in the grain during prolonged exposure.

After the irradiated grains are developed, the undeveloped silver bromide is dissolved in the fixing solution and removed from the emulsion. The emulsion is washed with water and dried.

After manifestation and fixation tracks of charged particles are visible under the microscope at magnification of several hundred times in the form of chains of black grains of metallic silver. If the grains are closely located, it is easy to distinguish the track, if far apart, it is difficult to separate the grains belonging to the track from the grains of the veil.

1.1.2. Properties of nuclear emulsions.

Nuclear emulsion differs from ordinary photographic emulsion in the small size and high density of grains in gelatin, the large thickness of the sensitive layer and high sensitivity, the low energy that must be expended to form a latent image in an individual grain.

Small grain size and proximity of neighboring grains to each other are necessary to confidently differentiate manifested grains belonging to the particle track from veil grains. The smaller the grains and the closer they are to each other, the better the spatial resolution of the emulsion and the easier it is to separate tracks belonging to different particles and to analyze a complex multi-particle event.

To increase the effective layer thickness, emulsion chambers are used, a set of layers several hundred microns thick each, stacked one on top of the other. After irradiation, each layer is shown separately. The total thickness of the layers can reach tens of centimeters. The main difficulty in the application of such cameras is the difficulty in identifying tracks of particles passing from layer to layer.

Emulsions contain mainly three groups of atoms far apart in atomic mass - H; C, N, O; Ag, Br - with very insignificant amounts of S, I, Au. The elemental composition of different emulsions is almost the same. All emulsions are close to each other with respect to nuclear interactions.

1.2. Classification of tracks

Secondary charged particles are divided into three classes depending on the velocity β (which is determined by ionization):

- **s-particles** - relativistic with c $\beta > 0.7,\ I < 1.4I_0,$

their number n_s , I_0 - ionization on the tracks of primary particles;

- **g-particles** - gray track, $0.24 < \beta \leq 0.7,\ I \geq 1.4I_0,$

their number n_g, proton energy $26\ MeV < E_p < 400\ MeV;$

- **b-particles** - black tracks, $\beta \leq 0.24$, their number is n_b, $E \leq 26\ MeV$ (*residual range < 3000 μm*).

The star type is written as $n_b + n_g + n_s$, with $n_b + n_g = n_h$ - the number of strongly ionizing particles.

Relativistic particle tracks are separated from gray tracks (near the boundary $I \sim (1.45 - 2.0) I_0$) by grain count on the studied track and on the track of the primary particle (at the same depth in the emulsion). Black tracks are separated from gray tracks (near their interface) by the residual run length ($R_b \leq 3000\ \mu m$).

Due to the high spatial resolution of nuclear trek emulsions, recoil nuclei and β-electrons are also recorded.

Since at high energies nuclear interactions with large n_s , n_g, n_b, as well as an increased background of extraneous particles are observed, a special ocular scale and a special form on which the location of all tracks in a conventional scale are plotted are used to study and determine the type of star. The type of star is determined before measuring angles on special measuring microscopes for nuclear research KSM-1. The goniometer of this microscope effectively helps to exclude the background of extraneous particles. MBI-9 microscopes can also be used to determine the star type.

1.3. *Classification of events*

To characterize the interactions on nuclei, there is a technique for separating interactions with light and heavy nuclei, based on the presence of short-range particles ($R_{min} \leq R_{cr}$) on light nuclei and their absence on AgBr nuclei, at low excitations of the nucleus, due to the Coulomb barrier, as well as on the dependence of the inelastic hadron interaction cross section on the atomic number ($A^{0.7}$ for protons, $A^{0.75}$ for π-mesons).

To establish the critical particle range R_{cr} , it is necessary to study the characterization of slow particles by range for high energy nuclear interactions in conventional BR, BR2, Ilford G5 nuclear photoemulsions as well as in BR2x4u emulsions with increased content of light nuclei.

As a result of detailed analysis of experimental and literature data, the value of $R_{cr} = 80\ \mu m$ and $R'_{cr} = 120\ \mu m$ for conventional emulsions of BR, BR 2, Ilford C-5 and BR2x4u, respectively, were obtained and the following separation criteria for conventional emulsions were established.

All events with $I < n_h \leq 6$ with $n_b \geq I$, as well as events of the type $0 + 0 + n_s + r.n.$ (recoil nucleus) and $0 + I + n_s + r.n.$ are classified as interactions on CNO nuclei - this group is labeled “L”.

The interactions on Ag, Br nuclei include:

- all events with $I < n_h \leq 6$ at $n_b \geq I$ and $R_{cr} > 80\ \mu m$, as well as events $0 + I + n_s$ with gray track back in the laboratory system and $0 + 2 + n_s$ - this group is labeled “T_1”;

- all events with $n_h \geq 7$ is the “T_2” group; it accounts for about half of all interactions on Ag, Br nuclei.

To characterize the interactions on the CNO nuclei and AgBr, the groups “L” and “T”=“T_1”+“T_2” were complemented statistically by interactions on hN nucleons according to the cross sections, with hN events accounting for about 30% of all interactions on CNO nuclei and about 10-15% on AgBr nuclei. For emulsions of ordinary composition, “L” events account for (17±1)% of all hA interactions in the energy region 20-400 GeV.

1.4. Simulation range-energy relations for α-particles in NTE

The Stopping and Range of Ions in Matter (SRIM) is a collection of software packages which calculate many features of the transport of ions in matter. This software works over a relatively wide energy range from 10 eV/amu up to 2 GeV/amu and uses a full quantum mechanical treatment of ion–atom collisions. Typical applications include: ion stopping and range in targets; ion implantation; sputtering; ion transmission; ion beam therapy.

Most aspects of the energy loss of ions in matter are calculated in SRIM. SRIM includes quick calculations which produce tables of stopping powers, range and straggling distributions for any ion at any energy in any elemental target. More elaborate calculations include targets with complex multi-layer configurations.

Ion beams are used to modify samples by injecting atoms to change the target chemical and electronic properties. The ion beam also causes damage to solid targets by atom displacement and may knock out target atoms, a process called ion sputtering. The calculation of sputtering, by any ion at any energy. Ion beams can be followed through

mixed gas/solid target layers, such as occurs in ionization chambers or in energy degrader blocks used to reduce ion beam energies.

Using the SRIM software, we simulated the passage of a-particles with kinetic energy in the region of 1 - 10 MeV through the Ilford G5 nuclear track emulsion volume available in the standard SRIM library. Figure 2 shows the dependence of the kinetic energy of the E_{kin} fragment on the range L of the a-particle obtained from SRIM modelling.

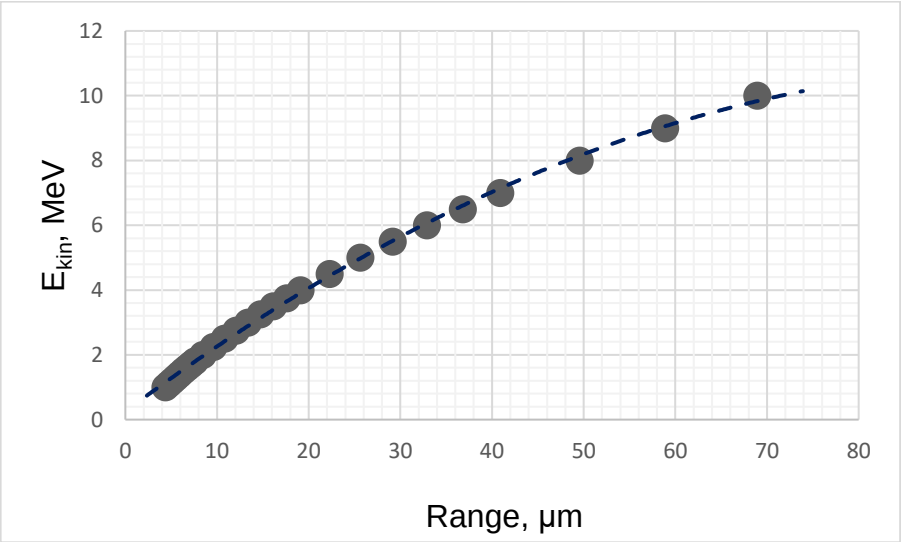

Figure 2. Dependence of the kinetic energy of the E_{kin} fragment on the range L of the a-particle obtained from SRIM modeling. The curved line is the fit of the dependence of the approximating function (1).

The model dependence of the kinetic energy of the E_{kin} fragment on the range L was approximated by a function:

$$E_{kin}(L) = -0{,}001 \cdot L^2 + 0{,}2114 \cdot L + 0{,}2491 \qquad (1)$$

2. *Irradiation of nuclear emulsion prototypes by relativistic muon beam at the COMPASS CERN*

Irradiation of nuclear emulsions produced by scientific production association (SPA) “Slavich” was performed on a muon beam (μ^-) with an energy of 160 GeV at the COMPASS facility in CERN in 2014. One of the purposes of irradiation was to test photoemulsion layers produced by SPA “Slavich”, Pereslavl-Zalessky, Russia under conditions of high energies, beam intensities and a long interval between irradiation and developing stages. Nuclear emulsion layers were placed in the beam halo (25 cm from the axis), where the muon intensity was 106 particles/cm^2 per spill. In 2017, an additional irradiation of 200 μm thick layers was performed. The irradiation was performed to

increase the statistics of $\mu+^{12}C\rightarrow 3\alpha$ interactions, which in the previous case amounted to 72 events. Such a small the number of events found is due to the inelastic interaction cross section of muons with matter ~ 10^{-6} - 10^{-5} barn (10^{-24} cm^2) multiplied by the probability of the $^{12}C\rightarrow$ 3α channel and the nature of the irradiation. The muon flux was directed perpendicular to the plane of the emulsion layer (transverse irradiation of emulsions) in order to reduce the additional background from muon tracks, which is much higher in the case of longitudinal irradiation. Scanning of the photoemulsion layers and search for $^{12}C\rightarrow 3\alpha$ events were carried out at the JINR LHEP. The track characteristics (energy, momentum) of the formed α-fragments were determined on the basis of the run-energy relation using SRIM modeling. Fragment departure angles were measured directly on the microscope at the JINR LHEP.

3. Search for inelastic interactions of muons with light nuclei

Depending on the tasks of emulsion experiments, scanning of nuclear emulsions can be performed by the methods “by track”, “by area” or “by strips”. Track-by-track viewing method is realized in tracing the tracks of the studied particles from the place of entry into the emulsion layer, to the interaction, or to the place of track exit from the emulsion. Viewing “by track” makes it possible to follow the particle and detect all interactions with high accuracy. The essence of the method of viewing “by area” is to search for events from the reaction channels of interest sequentially in the entire volume of the emulsion layer, in all layers of the emulsion. This method is effective when searching for events with a large multiplicity of formed tracks. A faster set of statistics (in comparison with the “track-by-track” search) is also provided by the “stripe-by-stripe” search method. The procedure of searching “by stripes” differs from the “by area” viewing in that the viewing is performed in certain parts of the emulsion layer at a certain distance from each other so that the scanned areas resemble stripes. The search for events by this method relies on the peculiarities in the location of tracks coming from the interaction vertex.

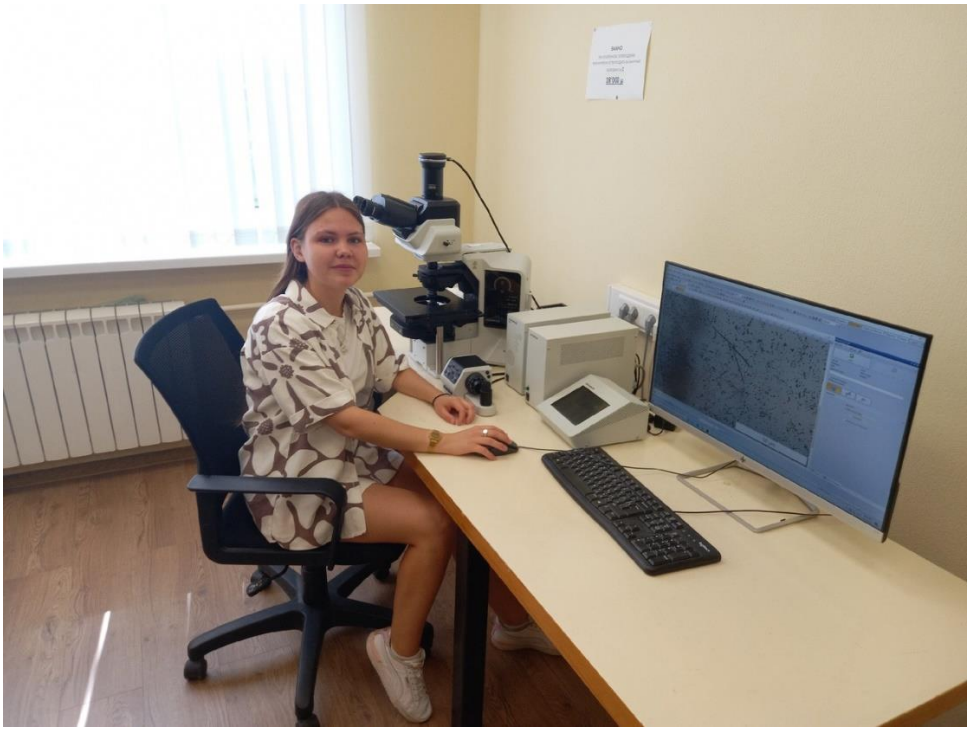

Figure 3. Searching for events in the volume of nuclear emulsion using the motorized microscope Olympus BX63

The statistics of the interaction of muons with emulsion nuclei obtained by viewing 30 bands with a total area of 27 cm^2 was studied. When viewing this area, 309 events were found.

Number of tracks in the event	Number of events
2	*102*
3	*125*
4	*53*
5	*29*

Table. 1. Separation of events by number of tracks

We are only interested in events with three tracks emanating from a single vertex, whose length does not exceed 80 μm. An example of the events under consideration is shown in Figure 4. It is worth noting that the observed events are located close to the boundary of the sensitive volume of the photoemulsion and the glass base. Such events, the vertexes of which are not observed in the volume, we refer to the events of interaction of muons with the substance of the glue and refer to the interaction of muons with carbon in the glue base. Thus, we will not consider these events for the reason that for further work we need events that occurred in the volume of the sensitive material.

When viewing the array of found events, we selected real events of interaction of muons with carbon nuclei in the substance of nuclear photoemulsion, measured the coordinates of the beginning and end of the alpha particle run, thus restoring the event in 4π geometry. This information allows us to know the real range of the alpha particle in the substance of the nuclear photoemulsion. Knowing the range, we can estimate the kinetic energy of the alpha particle by means of approximation with SRIM.

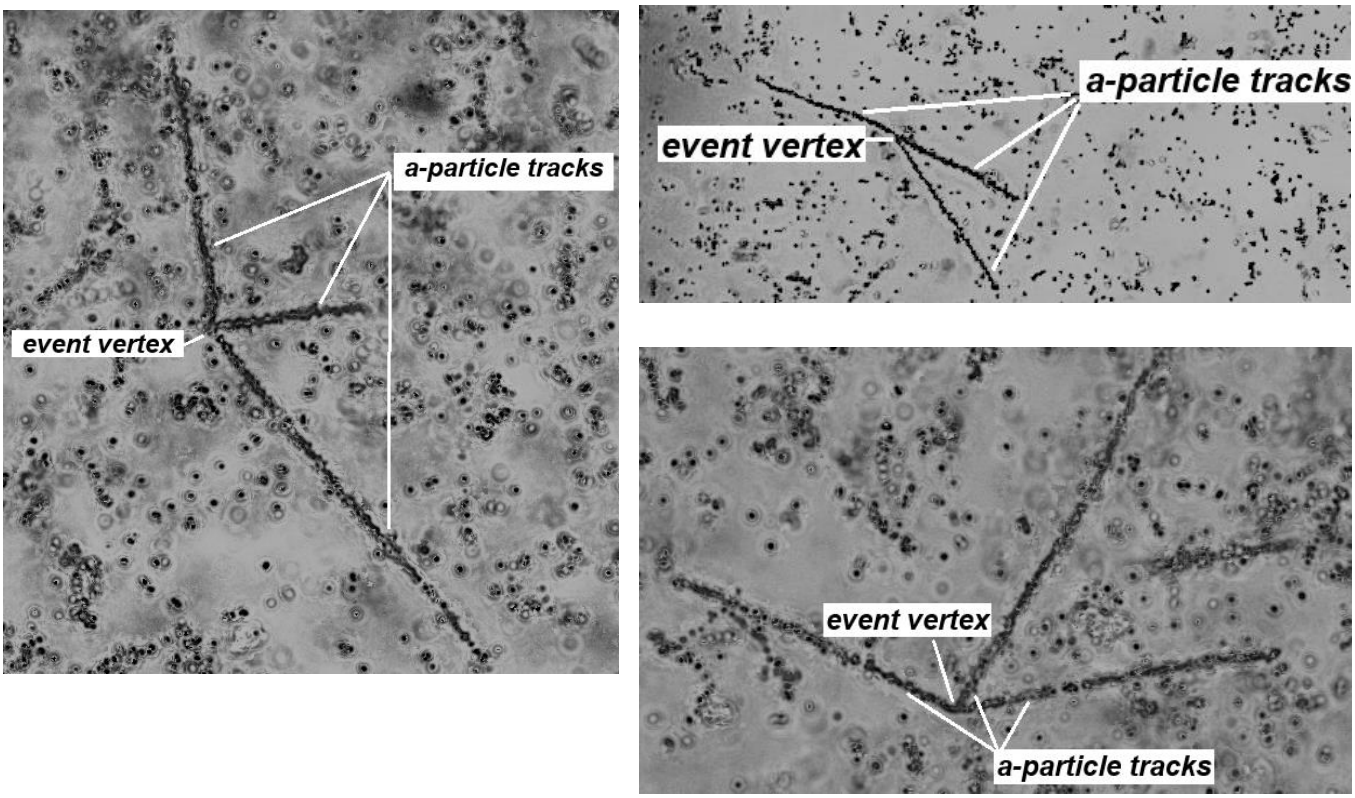

Figure 4. Images of track-forming events α -particles at μ+^{12}C→3α

4. Measurements and analysis

Measurements of the found events were performed on a KSM-1 optical microscope using an oil-immersion objective. The thickness, vertex and end-of-track coordinates for each α -particle emitted from the vertex of the event were measured.

The mean α -particle track thickness in events with three α -particles corresponds to $< d >= 0.9\ \mu m$ with a mean square deviation $\sigma_d = 0.2\ \mu m$. Distribution of the track thickness α -particles in μ+^{12}C→3α reaction events is shown in Figure 5.

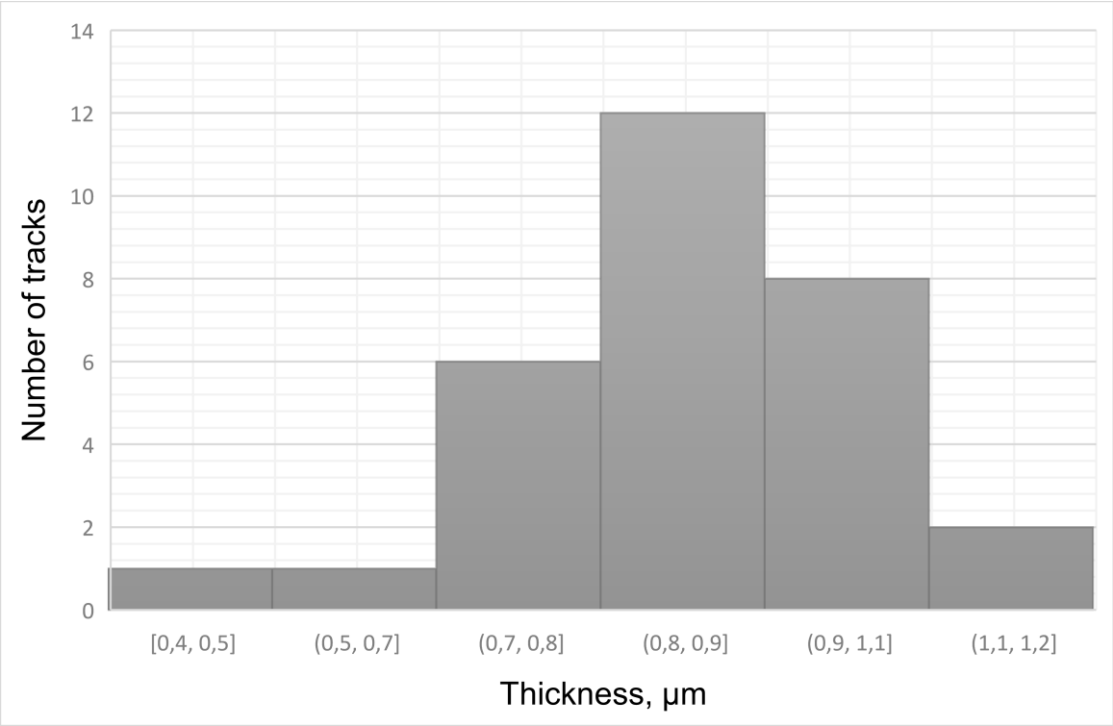

Figure 5. Distribution of the track thickness α -particles in $\mu^+ {}^{12}C \rightarrow 3\alpha$ reaction events.

The range of α -particles in the NTE was determined as $L = \sqrt{\Delta x^2 + \Delta y^2 + (k\Delta z)^2}$ where Δx, Δy and Δz are the differences of the coordinates of the event vertex and the end of the α -particle track, k is the shrinkage factor of the emulsion layer determined by the ratio of the initial (production) thickness to the thickness after chemical development. The average length of the measured tracks in events with three α -particles is $< L > = 25.1$ μm, and the standard deviation from the mean $\sigma = 6.9$ μm.

Substituting the measured α -particle runs in the $^{12}C \rightarrow 3\alpha$ events into the run-energy functional relationship (1), we can recover the total kinetic energies of α -particles stopped in the emulsion. In figure 6 shows the distributions for the kinetic energies of α -particles recovered in this way and for their total energy release in the event $\mu^+ {}^{12}C \rightarrow 3\alpha$.

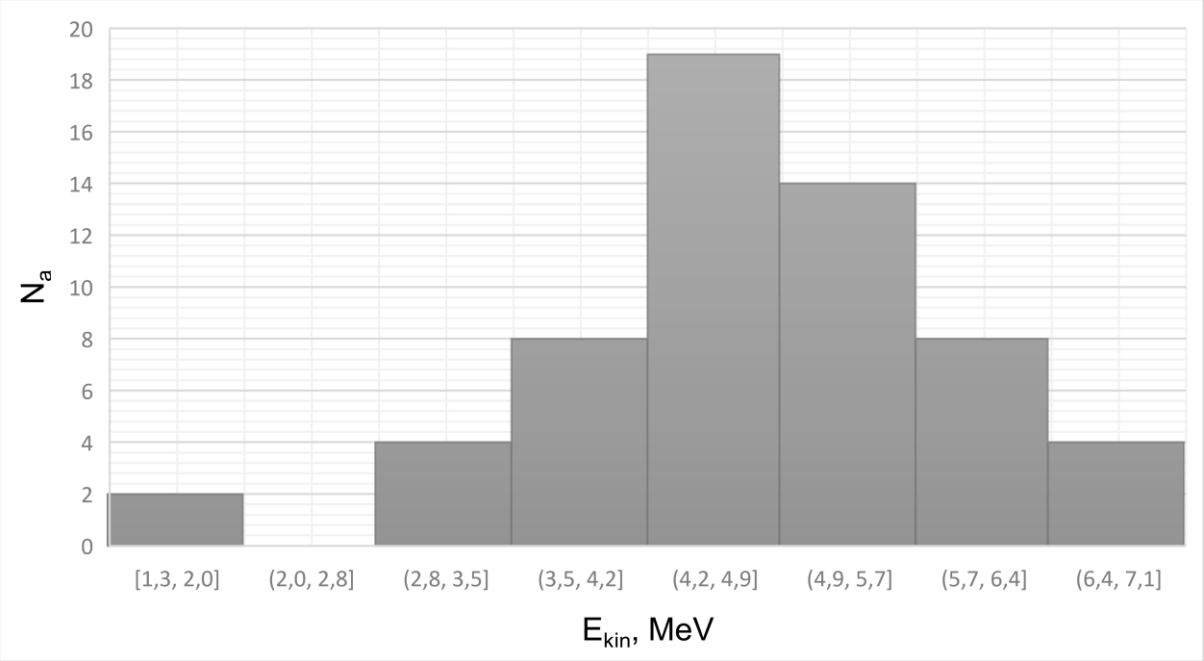

Figure 6. α -particle distribution over reduced energies α -particles in $\mu^+ {}^{12}C \rightarrow 3\alpha$ reaction events.

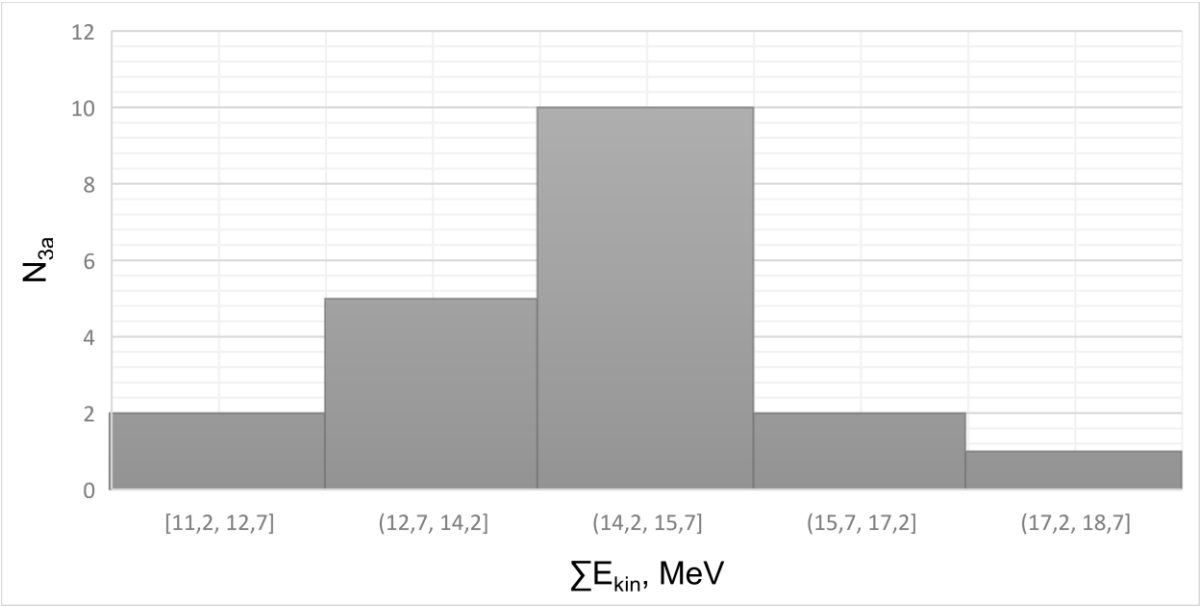

Figure 7. The total distribution of the reduced energies of 3α -particles in the $\mu^+ {}^{12}C \rightarrow 3\alpha$ reaction events.

The mean single-particle kinetic energy in events with three α-particles is $< E_{kin} > = 4.9\ MeV$, and the standard deviation from the mean value $\sigma_{E_{kin}} = 1.1\ MeV$. The mean total energy release in events with three α-particles is a value $< \sum E_{kin} >= 14.6\ MeV$, the corresponding standard deviation from the mean value $\sigma_{\sum E_{kin}} = 1.5\ MeV$.

5. Conclusion

During my participation in the START programme at the Veksler and Baldin Laboratory of High Energy Physics JINR, I learned how to analyze relativistic interactions of muons with nuclei by means of the nuclear track emulsion method. This method is widely used in the field of registration of elementary particles and decay reactions. The main advantage of nuclear emulsions is the best space resolution.

I investigated the events with observed three alpha particle tracks as a result of the electromagnetic dissociation of the excited nucleus of the ^{12}C target in interaction with relativistic muons. For this purpose, I studied the technique of scanning and searching for events in the volume of nuclear emulsion using the optical microscope MBI-9, motorized microscope Olympus BX63, learnt to work with the viewing logbook and analyze the found events. Then I've measured the real alpha particle range and track thickness on a KCM-1 microscope. I reconstructed the kinetic energies of alpha particles using the SRIM software that models the alpha particles' passage through the substance of the nuclear emulsion. As a result of the analysis of 20 events of the $\mu + {}^{12}C \rightarrow 3\alpha$ reaction, was obtained that the mean α -particle track thickness in events with three α-particles corresponds to $< d >= 0.9\ \mu m$ with the standard deviation from the mean $\sigma_d = 0.2\ \mu m$. The average length of the measured tracks in events with three α -particles is < L > = 25.1 μm with $\sigma_L = 6.9\ \mu m$. The mean single-particle kinetic energy in events with three α-particles is $< E_{kin} >= 4.9\ MeV$ with $\sigma_{E_{kin}} = 1.1\ MeV$. The mean total energy release in events with three α-particles is a value $< \sum E_{kin} >= 14.6\ MeV$ with $\sigma_{\sum E_{kin}} = 1.5\ MeV$.

The experimental material I received will complement the already existing database of the Becquerel experimenter on the study of fragmentation of light target nuclei induced by the relativistic hadrons and muons.

6. References

1. Freier P., Lofgren E.Jo., Ney E.P., Oppenheimer F., Bradt H.L. and Peters B. // Phys. Rev. 1948. V. 74. No. 2. P. 213.

2. Yariv Yo. and Fraenkel Z. // Phys. Rev. C. 1979. V. 20. No. 6. P. 2227.

3. Kaufman S.B. and Steinberg E.P. // Phys. Rev. C. 1980. V. 22. No.1. P.167.

4. Hüfner J. // Phys. Rep. 1985. V. 125. No. 4. P. 129.

5. Sümmerer K., Brüchle W., Morrissey D.J., Schädel M., Szweryn B. and Weifan Y. // Phys. Rev. C. 1990. V. 42. No. 6. P. 2546.

6. Cherry M.L., Dabrowska A., Deines-Jones P., Hoynski R., Nilsen B.S., Olszewski A., Szarska M., Trzupek A., Waddington C.J., Wefel J.P. et al. // Eur. Phys. J. C. 1998. V. 5. P. 641.

7. Khushnood H. et al. // Proceedings of the DAE Symp. on Nucl. Phys. 2014. V. 59, P. 748.

8. Zaitsev A.A. and Zarubin P.I. // Phys. At. Nucl. 2019. V. 82, P.1225.

9. Artemenkov D.A., Bradnova V., Kashanskaya O. N., Kondratieva N. V., Kornegrutsa N. K., Mitsova E., Peresadko N. G., Rusakova V. V., Stanoeva R., Zaitsev A. A., Zarubina I. G. and Zarubin P. I.// Phys. At. Nucl., 85(6):528 539, 2022.

10. Tretyakova M. I.//Akademiya Nauk USSR Ordena Lenina Fizicheskiy Inst. Imeni P. N. Lebedeva (Moscow, USSR). 1984.

11. Powell S., Fowler P., Perkins D. Study of elementary particles by the photographic method. Moscow: Foreign Literature Publishing House, 1962.

12. Abramov A.I., Kazansky Yu.A., Matusevich E.S. Fundamentals of experimental methods of nuclear physics. Moscow: Energoatomizdat, 1985.

13.S. M. Othman, M. T. Ghoneim, M. T. Hussein, H. El-Samman, A. Hussein // International Journal of Modern Physics E Vol. 27, No. 1 (2018)

14. Kuznetsov D.A. Study of the splitting of carbon nuclei under the action of ultrarelativistic muons. Smolensk: Smolensk State University. 2022

15. http://www.srim.org/index.htm

16. http://becquerel.jinr.ru/index.html